

Article

Toward Self-Healing Coatings: Bacterial Survival and Calcium Carbonate Precipitation in Acrylic and Styrene–Acrylic Model Paint Films

Matthew E. Jennings¹, George J. Breley^{2,3}, Anna Drabik², Chinnapatch Tantisuwanno⁴, Maria A. Dhinojwala², Anuradha Kanaparathi¹ and Hazel A. Barton^{2,3,5,*} 

¹ Department of Biology, Wilkes University, Wilkes-Barre, PA 18766, USA; matthew.jennings@wilkes.edu (M.E.J.)

² Department of Biology, University of Akron, Akron, OH 44325, USA; gjb55@uakron.edu (G.J.B.); annadrabik217@gmail.com (A.D.)

³ Integrated Bioscience, University of Akron, Akron, OH 44325, USA

⁴ School of Polymer Science and Polymer Engineering, University of Akron, Akron, OH 44325, USA

⁵ Department of Geological Sciences, University of Alabama, Tuscaloosa, AL 35487, USA

* Correspondence: hbarton1@ua.edu

Abstract: Engineered living materials (ELMs) incorporate living material to provide a gain of function over existing materials, such as self-repair. The use of bacteria in ELMs has been studied extensively in concrete, where repair can be facilitated by bacterial ureolytic calcium carbonate (CaCO₃) precipitation; however, the study of bacteria in other construction materials is limited. We examined the ability of bacterial species to survive in common latex binder chemistries, a model paint formulation, and through the film-forming process. The longest survival was by bacterial spores of *Bacillus simplex* str. GGC-P6A, which survive in latex emulsions, a liquid coating composition, and in a dried film for >28 days. Surprisingly, our data show that non-spore-forming *Escherichia coli* survive at least 15 days in liquid composition, which appear to be influenced by the composition of the outer membrane, nutrient scavenging, and the ability to metabolize toxic acrylate. Spores of GGC-P6A were shown to grow in solid paint films from sites of damage, resulting in crack filling through carbonate precipitation, demonstrating the potential for self-repair through microbially mediated CaCO₃ precipitation without directed pH modification. These data suggest that a range of bacterial species, in particular members of *Bacilli*, may facilitate new applications of bio-augmented, self-healing coating systems.

Keywords: *Bacillus*; engineered living materials; calcium carbonate; paint; coatings



Citation: Jennings, M.E.; Breley, G.J.; Drabik, A.; Tantisuwanno, C.; Dhinojwala, M.A.; Kanaparathi, A.; Barton, H.A. Toward Self-Healing Coatings: Bacterial Survival and Calcium Carbonate Precipitation in Acrylic and Styrene–Acrylic Model Paint Films. *Buildings* **2024**, *14*, 1202. <https://doi.org/10.3390/buildings14051202>

Academic Editor: Mizan Ahmed

Received: 6 March 2024

Revised: 11 April 2024

Accepted: 17 April 2024

Published: 24 April 2024



Copyright: © 2024 by the authors. Licensee MDPI, Basel, Switzerland. This article is an open access article distributed under the terms and conditions of the Creative Commons Attribution (CC BY) license (<https://creativecommons.org/licenses/by/4.0/>).

1. Introduction

Research into the use of microorganisms to perform limited self-maintenance and repair in construction materials, known as engineered living materials (ELMs), has received substantial interest in recent years [1–3]. Bacteria with specific phenotypes have the potential to repair damage and prolong the operational life of such materials [1,3–5]. To date, research related to ELMs in construction repair has been confined almost exclusively to concrete, where two mechanisms of microbially induced calcite precipitation (MICP) have been used to repair cracks and maintain the structural integrity of concrete [6–8]. The first approach uses ureolytic bacteria to catalyze the hydrolysis of urea to carbon dioxide and ammonia, increasing the pH and the subsequent saturation index for calcium carbonate (CaCO₃) [1,7,9]. In the second approach, an organic calcium salt (such as calcium lactate) [10], or inorganic calcium salt (such as calcium chloride) [3], are embedded along with the bacteria in the concrete to provide nutrients for growth and metabolic CaCO₃ precipitation, although the high amount of organic carbon that must be embedded along with the bacteria (up to 50% weight) dramatically reduces the tensile strength of the concrete [11]. Extensive work examining the potential for microbial self-healing in

concrete and other solid building materials such as polymers has been conducted; however, comparatively little work has examined the potential for microbially mediated repair in surface coatings [12,13].

It is estimated that $\sim 3.3 \times 10^{10}$ L of surface coatings are manufactured worldwide [14]. Coating is the general term for film-forming materials that provide environmental protection, and encompasses high-performing products for concrete, metal, and other non-architectural surfaces. Paint refers to latex-based coatings suitable for the interiors and exteriors of homes and commercial buildings [14] and are applied to decorative surfaces with the use of color and texture. In construction, coatings are primarily used for protection, shielding metal and wood surfaces from environmental factors, such as UV radiation, moisture (precipitation), and physical wear and tear [14]. These coatings generally contain three major components that vary depending on the application: a polymeric binder (typically acrylic or styrene–acrylic latex) that serves as glue to hold together the pigments, such as CaCO_3 , titanium dioxide, or silicate clays, which provide color and enhance durability, and the solvent (typically water for latex-based paints) in which the components are dispersed [14]. Additional functional additives include a thickener to provide viscosity appropriate for the application (brushes, rolling, or spraying), surfactants to limit foaming, and biocides to prevent microbial degradation of the emulsion and maintain shelf-life [14]. This mix is used as a protective coating over the surface, although when damaged (through scratching, gouging, abrasion, cracking, or age) this protection is compromised, and a new coating must be applied. If a self-healing ELM coating could be developed, where minor damage to the film could be repaired without adding the additional layers needed, this could provide considerable cost and maintenance savings, while reducing structural monitoring.

Self-healing mechanisms have been studied for many years as a way to extend the life of coatings and reduce the maintenance costs associated with re-application [15]. Current self-healing technologies for paints are based on two approaches: the first involves the incorporation of capsules in the paint that, when broken, fill the damage [16–18], and the second involves a more complicated vascular structure that, when broken, allows the flow of material to fill cracks [19,20]. Both approaches are based on the mass movement of material from one place to another, weakening the coating at locations other than the site of original damage [19].

High levels of CaCO_3 (up to 30% solids in many coatings) as a pigment provide the potential for MICP to be used to repair damage in a microbially mediated self-healing paint; however, the use of existing approaches, such as ureolysis, is limited due to the already high pH in formulated coatings, along with the malodor issues that would be associated with the production of ammonia in an interior paint. Bacteria can facilitate precipitation of CaCO_3 through a variety of mechanisms other than ureolysis [21,22]. Our past work on bacteria isolated from caves has demonstrated the ability of bacteria to excrete potentially toxic levels of Ca^{2+} using the ChaA transporter protein [23]. To overcome the thermodynamic barrier against pumping out Ca^{2+} , the cell modifies the extracellular environment through buffering with HCO_3^- , altering the pH and leading to spontaneous precipitation of CaCO_3 [23,24]. If microbial CaCO_3 precipitation could be incorporated into a paint or coating, it may be possible for the precipitated material to heal cracks in the coating. In this paper, we examine the ability of bacteria with strong precipitation phenotypes, isolated from Ca^{2+} -rich cave environments, to survive in the water-based acrylate and styrene emulsions commonly used in household paints [14]. Of the species screened, we examined the ability of a long-surviving *Bacilli* species embedded within a model paint film to grow and repair damaged paint films. By exploring some of the phenotypes that would promote survival in the model bacterial species, *E. coil*, our results allow for a preliminary understanding of how survival in paint formulations could be affected by cellular architecture and metabolism.

2. Materials and Methods

Cultures and growth conditions. All environmental strains used in this study were originally collected and identified as described in Banks et al. [23], with all incubations carried out at room temperature (21 °C). The *E. coli* knockout strains used in this study were obtained from the Keio collection, a collection of *E. coli* strains where the target gene is replaced by a kanamycin resistance cassette [25]. Liquid cultures were shaken at 85 rpm on a Jeio Tech Lab Companion SKC 6200 orbital shaker (Billerica, MA, USA). Unless otherwise stated, growth was carried out on half-strength TSA, containing 15 g/L trypticase soy broth and 15 g/L agar, or half-strength TSB containing 15 g/L trypticase soy broth (BD Difco, Franklin Lakes, NJ, USA). The B4 media contained 4 g/L yeast extract, 10 g/L glucose, and 15 g/L agar, pH 7.2, with 2.5 g/L calcium acetate added after autoclaving to prevent precipitation [26,27]. The minimal B4 media was made the same way but lacked the added calcium acetate. All media were sterilized in a SR24D SV autoclave at 121 °C for 15 min (Consolidated Sterilizer Systems, Boston, MA, USA).

Spore suspensions of strain *B. simplex* GGC-P6A were prepared by growth in TSB for 9 days. The mixed cell/spore suspension was then pelleted at 2700× *g* for 10 min in a Sorvall XTR centrifuge (Thermo Fisher Scientific, Waltham, MA, USA) and resuspended in 25 mL sterile H₂O with shaking for an additional 7 days. Microscopic cell counting using an Olympus BX53 light microscope (Shinjuku, Japan), following malachite green (0.5%) staining with a safranin (2.5%) counterstain, confirmed that the final suspension contained > 99.8% spores. Vegetative cells and spore suspension CFUs were confirmed by serial dilution and plating on TSA.

Binder chemistry and model coating composition. Unless stated, all reagents were purchased from Sigma Aldrich and used as received. Stock solutions of Acrysol TT-935 were purchased from Dow Chemical (Midland, MI, USA). ALBAFIL S10 (70% CaCO₃, 700 nm particle size) was obtained from Specialty Minerals (Adams, MA, USA). Upon arrival, the ALBAFIL was autoclaved at 15 psi for 15 min prior to use. The general scheme of binder synthesis is shown in Supplemental Figure S3.

MBF1 was prepared using a semi-continuous emulsion polymerization with an ammonium persulfate initiator and a monomer mixture including 41.0% styrene, 10% methyl methacrylate, 43.5% 2-ethyl hexyl acrylate, 3.0% methacrylic acid, and 2.5% diacetone acrylamide. The monomers and initiator were fed into a reactor containing an additional initiator at 80 °C over a period of 3 h and stirred for an additional 30 min. Then, 20% terbutylhydroperoxide and 20% sodium metabisulfate were added as separate solutions over 45 min at 65 °C to ensure monomer consumption. The liquid was cooled to room temperature and adjusted to a pH of 8.5 with ammonium hydroxide. A mixture of 20% adipic dihyrazide was added and then the solution was filtered.

MBF2 was prepared using a semi-continuous emulsion polymerization with an ammonium persulfate initiator and a monomer mixture including 58% methyl methacrylate, 37% butyl acrylate, 2.5% methacrylic acid, and 2.5% diacetone acrylamide. The monomers and initiator were fed into a reactor at 80 °C containing an additional initiator over a period of 2.5 h and stirred for an additional 30 min. Then, 20% terbutylhydroperoxide and 20% sodium metabisulfate were added as separate solutions over 45 min at 65 °C to ensure monomer consumption. The liquid was cooled to room temperature and adjusted to a pH of 8.5 with ammonium hydroxide. A mixture of 20% adipic dihyrazide was added and then the solution was filtered.

MBF3 was prepared using a semi-continuous emulsion polymerization with an ammonium persulfate initiator and a monomer mixture including 37.0% styrene, 9.5% methyl methacrylate, 45.5% butyl acrylate, and 8.0% methacrylic acid. The monomers and initiator were fed into a reactor containing an additional initiator at 78 °C over a period of 3 h and stirred for an additional 30 min. Then, 20% terbutylhydroperoxide and 20% sodium metabisulfate were added as separate solutions over 45 min at 65 °C to ensure monomer consumption. The liquid was cooled to room temperature and adjusted to a pH of 8.5 with

ammonium hydroxide. A mixture of 20% zinc oxide was added and then the solution was filtered.

Bacterial survival assays. To examine survival in raw materials, 100 μL of a 3 mL overnight culture in TSB was used to inoculate 3 mL of MBF1, MBF2, and MBF3 before shaking at 85 rpm for 24 h, whereupon 100 μL samples were spread on TSA. Survival was recorded as positive/negative growth after 5 days. Long-term survival of GGC-P6A in binders was carried out in triplicate, although initial cell numbers were recorded by serial dilution of the inoculated binder on day 0, with cell survival recorded at 2, 7, 14, 21, and 28 days. The percent survival was calculated by averaging cell survival numbers at each time point, compared to the calculated CFU/mL at day 0 (recorded as % survival).

The model paint was prepared using 20 mL of the MBF1 binder, 1.6 mL ALBAFIL S10, 0.2 mL TT-935, and 18.2 mL sterile H_2O and inoculated on day 0 with either GGC-P6A vegetative cells or spores. CFU values were measured. CFU values were measured on day 2, 7, 14, 21, and 28. The paint films were prepared using the model paint, inoculated as described, with 10 mL volumes pulled down immediately onto non-stick polypropylene mats using a Leneta WC-1670 Wire-Cator (Mahwah, NJ, USA). The film was allowed to dry overnight in a laminar flow hood and cut into 25 mm-diameter coupons using a sterile hole punch (Fiskars, Helsinki, Finland). Coupons were then stored in sterile Petri dishes before plating on B4 media for growth. CFUs were calculated as the total cell number in the inoculated volume of the disk (22 μL) and emergent colonies counted by backlighting of the film. Survival was calculated as percentage survival compared to the initial inoculum on day 0.

Microscopy. Carbonate precipitation was monitored using an Olympus BX60 microscope using an DP73 camera attachment and cellSens v1.11 image capture (Olympus, Shinjuku, Japan). For scanning electron microscopy (SEM) analysis, 1 cm^2 squares were excised from dry paint films and coated with iridium using a Cressington 208HR Sputter Coater (Watford, UK). The thickness of the coating was estimated at 3 nm using the internal thickness monitor included with the coater. Images were captured using a Hitachi S-4700 Field Emission SEM (Chiyoda, Japan) in the SE (secondary electron) mode at 5 kV.

Zeta Potential Assays. Strains were grown in 3 mL of LB (which supports the growth of *E. coli*) overnight. Cells were pelleted by spinning the cultures at 3500 rpm for five minutes at 4 $^\circ\text{C}$. Cell pellets were washed three times with 1 mM potassium phosphate buffer (PB) before being resuspended in 3 mL of PB buffer. The samples were diluted 1:10 before 1 mL was loaded into a Zetasizer Nano (Malvern Panalytical) for measurement.

3. Results

To determine the ability of bacteria to survive in paint, we first examined cell viability in paint binders. As commercially available emulsion polymers cannot be purchased without preservatives (biocide additives), three polymeric paint binders were synthesized (see materials and methods). The three emulsion polymers were chosen to include the major types of monomers used in paint binders [styrene–acrylic (MBF1 and MBF3) and acrylic (MBF2)] and cross-linking chemistries (Table 1) [14].

Table 1. Monomer and cross-linking chemistry of used polymers.

Polymer Name	Monomer	Cross-Linking Agent
MBF1	Styrene–acrylic	Diacetone acrylamide/adipic dihyrazide
MBF2	Acrylic	Diacetone acrylamide/adipic dihyrazide
MBF3	Styrene–acrylic	ZnO

Fifteen bacterial strains previously isolated from caves that display a strong calcifying phenotype were selected for analysis (summarized in Table 2), including Gram-negative/positive and spore-forming species [23]. Given the large number of strains examined in three separate latex binders, we used a rapid, qualitative screen for survival. Vegetative cells from an overnight culture were assayed for survival for 24 h at room

temperature (Table 2). All the tested strains survived in binder MBF1, ten survived in MBF2, and nine species survived in MBF3 (Table 2). It was interesting to note that survival in MBF1, a styrene–acrylic polymer, did not necessarily correlate with survival in the other styrene–acrylic polymer MBF3 (Table 2). There was also no consistency in species survivability; for example, only two of three *Brevundimonas* strains (GGC-D2A and GGC-D2B) survived in MBF2, while none survived in MBF3. Finally, the ability of the tested species to form spores did not demonstrate any increase in survival (Table 2).

Table 2. Qualitative survival of strains in three paint binders after 24 h.

Species/Strain ^{1,2}	Gram Stain	Spores	Binder Survival		
			MBF1	MBF2	MBF3
<i>Brevundimonas</i> sp. str. GGC-D13	-	-	+	-	-
<i>Brevundimonas</i> sp. str. GGC-D2A	-	-	+	+	-
<i>Brevundimonas</i> sp. str. GGC-D2B	-	-	+	+	-
<i>Microbacterium</i> sp. str. GGC-P11	+	-	+	+	+
<i>Microbacterium</i> sp. str. GGC-P14	+	-	+	+	+
<i>Microbacterium</i> sp. str. GGC-D18A	+	-	+	-	+
<i>Microbacterium</i> sp. str. GGC-D5	+	-	+	+	+
<i>Microbacterium</i> sp. str. GGC-P13	+	-	+	+	+
<i>Streptomyces</i> sp. str. GGC-D15	+	+	+	-	-
<i>Streptomyces</i> sp. str. GGC-D17D	+	+	+	+	+
<i>Bacillus</i> sp. str. GGC-P1	+	+	+	+	+
<i>Bacillus</i> sp. str. GGC-P3	+	+	+	-	+
<i>Bacillus</i> sp. str. GGC-P2A1	+	+	+	+	+
<i>Bacillus</i> sp. str. GGC-P4	+	+	+	-	-
<i>Bacillus simplex</i> str. GGC-P6A ³	+	+	+	+	-

¹ Isolated from Banks et al., 2010 [23]. ² Identified using 16S rRNA sequencing. ³ Speciation confirmed via FAME analysis.

We decided to quantify survival of *Bacillus simplex* str. GGC-P6A, which demonstrated the best survival after 24 h in both MBF1 and MBF2 (MBF3 was not used due to the loss of GGC-P6A viability at <24 h; Table 2). Commercial paints are often a complex mixture, which can consist of up to 60 different additives, including biocides (for example, see ref. [28]). We therefore developed a simplified formula to assay survival of GGC-P6A containing only latex binder, CaCO₃ pigment, thickener, and water. We exclusively used binder MBF1, which provided the best recovery rates for GGC-P6A. The CaCO₃ slurry was ALBAFIL S10, a commercial slurry that negated the need for additional dispersants or surfactants [14]. The commercial thickener, Acrysol TT-935, is only available containing the biocides methylchloroisothiazolinone (MCI) and methylisothiazolinone (MI) at ~0.3% wt/wt [29]. To limit the impact of the biocides, TT-935 was diluted with water to a working concentration of 1% vol/vol, giving a final concentration of 0.0015% MCI/MI. As adequate films could be created with this simple formulation, no coalescent was required [14]. The model paint was inoculated with GGC-P6A vegetative cells and viability was examined for 15 days (Figure 1).

Given that GGC-P6A is a spore former, we wondered whether this extended survival was due to sporulation and used purified spores in our assays to measure long-term survival. Unsurprisingly, spore survival was higher compared to vegetative cells (Figure 1). Spores do not require nutrients, since they are in a dormant state, and there was no decrease in spore number over the 28 days compared to the vegetative cells (Figure 1). We observed an increase in overall cell numbers above the initial inoculum (Figure 1); however, there was more variability in spore number than vegetative cells. We believe that these variations may be due to clumping of spores within the paint, although this would be challenging to examine. Nonetheless, these data indicate that GGC-P6A spores were clearly able to remain viable at high levels for at least four weeks post-inoculation (Figure 1) and are

the ideal method of inoculation to retain large amounts of viable cells in our artificial paint formulation.

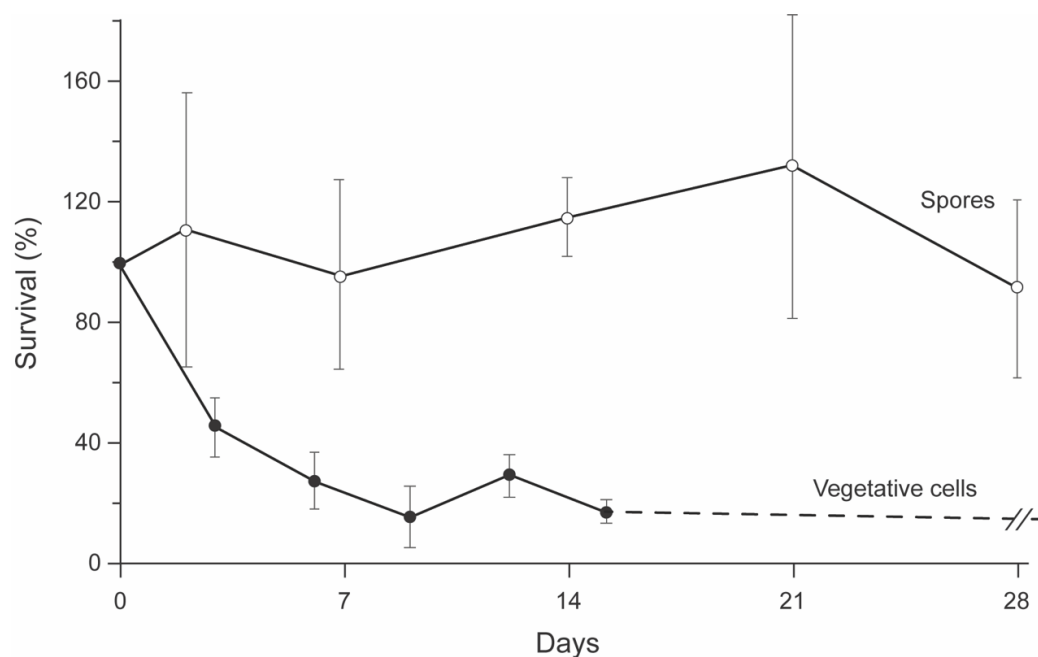


Figure 1. Survival of *B. simplex* str. GGC-P6A spores and vegetative cells in a model paint. Shown is the styrene–acrylic latex, MBF1, the color/opacity CaCO_3 slurry (ABBAFIL S10), and a thickening agent (Acrysol TT-945). Plotted values are the average of three replicates, with error bars representing standard deviation from the mean.

In order to be functional within an engineered coating, bacteria must be able to survive the process of drying and formation of a surface film. To determine the survival of GGC-P6A through this process while maintaining functionality (CaCO_3 precipitation), the liquid coating composition was inoculated with either GGC-P6A vegetative cells or spores. The coating was then immediately poured to create a film and allowed to dry for 24 h in sterile conditions to create coupons that could be cracked and placed on B4 media to facilitate growth, CaCO_3 precipitation, and examine potential crack filling. In the paint coupons inoculated with vegetative cells, bacterial growth was seen emerging across the surface and along the edges of the paint film within 3 days (Figure 2). After 7 days, the paint coupons demonstrated CaCO_3 precipitation, both on the surface of the film and along the edges of the cracks, with a noticeable carbonate front advancing ahead of bacterial growth (Figure 2). In places, this precipitated carbonate was able to occlude introduced cracks in the film (Figure 2B). When paint coupons inoculated with GGC-P6A spores were placed on B4 media, a similar pattern of growth and CaCO_3 precipitation was observed, suggesting that sporulation did not interfere with the precipitation phenotype.

The CaCO_3 precipitation assays on the paint films were carried out on B4 media, which contains $\text{Ca}(\text{C}_2\text{H}_2\text{OOH})_2$ as a calcium source; however, our original hypothesis was that the CaCO_3 within the coating would be sufficient to serve as a source of Ca^{2+} for CaCO_3 precipitation. To determine if this was the case, we created a B4 media that lacked $\text{Ca}(\text{C}_2\text{H}_2\text{OOH})_2$ (Figure 2D). When the paint coupons containing GGC-P6A vegetative cells were grown on this Ca^{2+} -free media, CaCO_3 precipitation could also be observed at the growth front, albeit at a reduced rate than observed on regular B4 media (Figure 2D). SEM images demonstrated vegetative cells emerging from, and following, cracks in the paint, or tracking along the edge of the paint film and onto the support media (Supplemental Figure S1) during the crack-filling process.

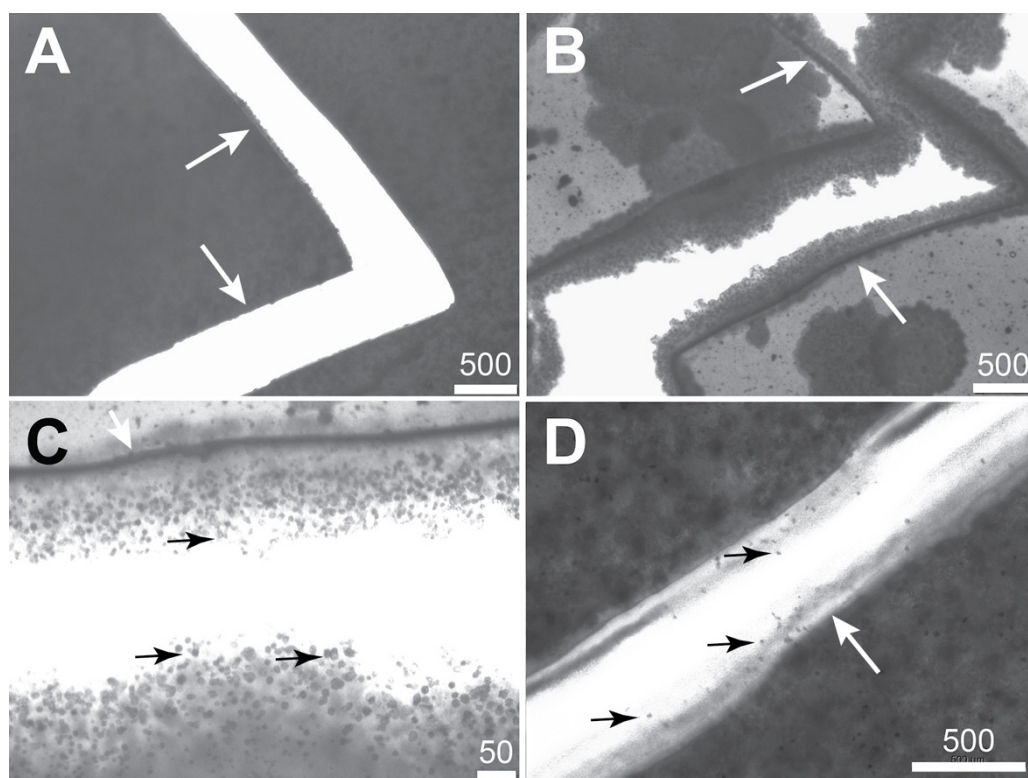


Figure 2. Growth of embedded GGC-P6A vegetative cells in model paint. (A) A crack was introduced into an MBF1 model paint film inoculated at 1×10^6 cells/mL GGC-P6A and placed on B4 support media. After 3 days of growth, bacterial growth (B) and CaCO_3 precipitation (C) was visualized by transmitted light on B4 media. (D) We also examined CaCO_3 precipitation when paint films containing embedded bacteria were plated on B4 lacking Ca^{2+} . The edge of the paint film is indicated (white arrows) along with opaque calcite crystals (small black arrows). All scale bars are in μm .

Once it was clear that the bacteria were able to survive the film-forming process and calcify, we wanted to examine their ability to survive long term in dried paint films. To do this, we inoculated the paint films with both vegetative cells and spores at a comparable level to our work in the liquid formulation: $\sim 1 \times 10^6$ CFU/mL. The films were then cut in 25 mm circles to standardize the volume of coupon used to $22 \mu\text{m}^3$ (the coupons were measured to be $\sim 45 \mu\text{m}$ in thickness; Supplemental Figure S2). These coupons were then either examined immediately or stored in empty, sterile Petri plates to assess long-term survival. When the coupons were incubated on B4 support media, there was significant microbial growth, and the film became confluent (Figure 3A). This made it difficult to quantify the actual number of colonies emerging from the film (Figure 3A), so we repeated the experiment by reducing the inoculum to 3.1×10^3 CFU/mL. While containing significantly fewer cells than the liquid formulations, this did allow us to observe quantifiable colony growth (Figure 3A). The coupons were plated on B4 support media at one-week intervals and the emergent colonies counted (Figure 3B). At day 0, the CFU/mL values obtained were comparable to the total number spores added (4.9×10^3 CFU/mL $\pm 0.4 \times 10^3$), suggesting that the creation of paint films did not have an immediate effect on viability. These data also validated this assay as a way of observing bacterial survival within the paint film. Over the course of the experiment, we saw a 50% reduction in the recovery of GGC-P6A spores in paint films by day 7, a number that appeared to remain stable over 28 days of the experiment, with no significant additional reduction (Figure 3B).

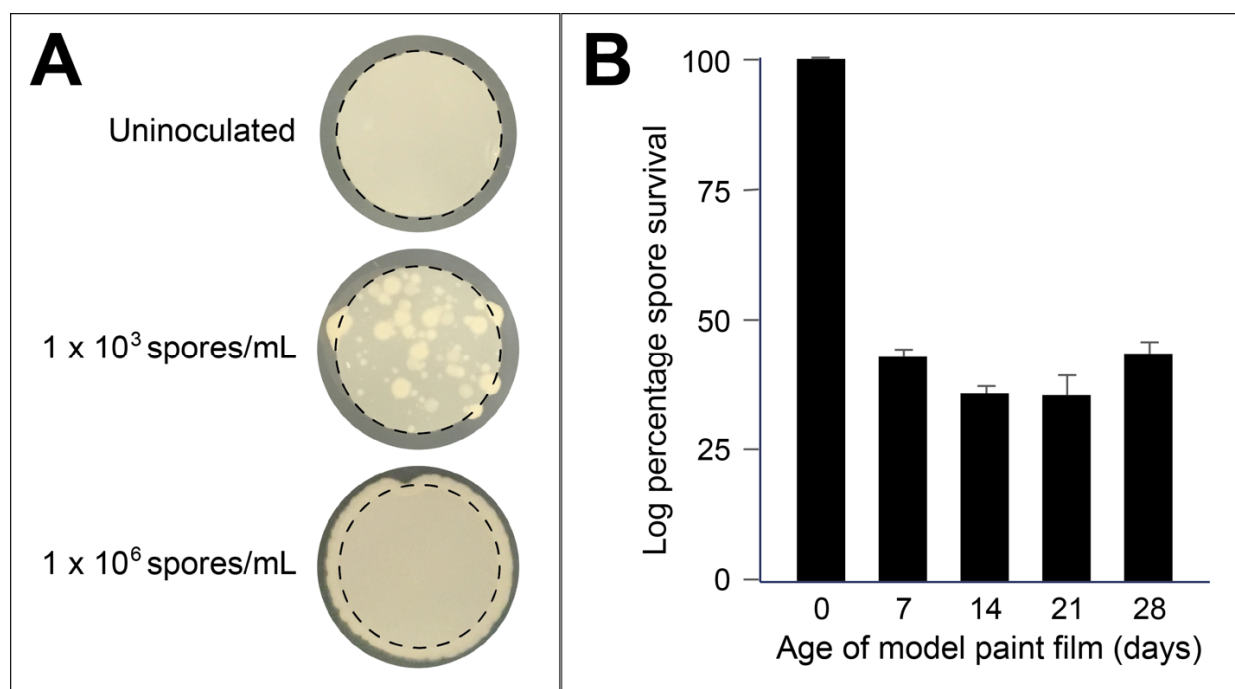


Figure 3. Long-term survival of GGC-P6A spores in model paint. Inoculated films were cut into standardized coupon sizes (A) and allowed to grow on B4 support media for 3 days before colonies were counted. Inoculation of $\sim 1 \times 10^6$ CFU/mL produced confluent growth, so long-term viability was carried out at 3.1×10^3 CFU/mL followed by colony counting ((A); the dashed line indicates the boundary of the paint coupon). Survival in dried paint films over 28 days (B) was standardized to percent survival from growth on day 0.

It was unsurprising that spore formers demonstrated long-term survival in the paint formulations; however, the use of spore formers somewhat limits the bacterial species that can be incorporated into coatings, or that are tractable for genetic enhancement. We had limited Gram-negative species in our cave isolates so decided to use *Escherichia coli* as a model species. We inoculated samples of model paint containing MBF1 with *E. coli* from a number of genetic backgrounds, including K-12, BL21 (DE3), and BW25113. To our surprise, not only did *E. coli* strains K-12 and BW25113 demonstrate low but persistent survival (Figure 4), but there was an inconsistency in the survival between strains, with *E. coli* strain BL21 (DE3) becoming unculturable after 3 d. Periodic sampling after 15 d demonstrated that cells remained culturable for at least 32 days for *E. coli* K-12 and BW25113, equivalent to the survival seen in GGC-P6A.

The *E. coli* strain BW25113 is a K-12 derivative, which lacks the ability to synthesize the complete *E. coli* O-antigen of LPS due to an insertion element present in *wbbL* [30,31]. BL21 (DE3) is a B strain, which also has a disruption in the O-antigen synthesis pathway, albeit at a different locus [30]. Genetic differences between the two backgrounds contribute to an outer membrane surface with significant structural differences [32], which could explain the difference in survival and affect cell interactions with the charged components of the polymer emulsions. While it was not possible to test any varying chemistry within the model paint formulation, we could compare the cellular zeta potential between strains as a general measure of surface chemistry in each *E. coli* strain (Figure 4). The largest difference in zeta potential was observed between BW25113 and K-12 (-28.7 and -64.4 mV, respectively), although survival between these strains was not significantly different after 6 d of growth (Student's *t*-test: $df = 2$, $p = 0.37$, Figure 2). Overall, no clear difference in viability was observed between the relative cell surface charge (Figure 4).

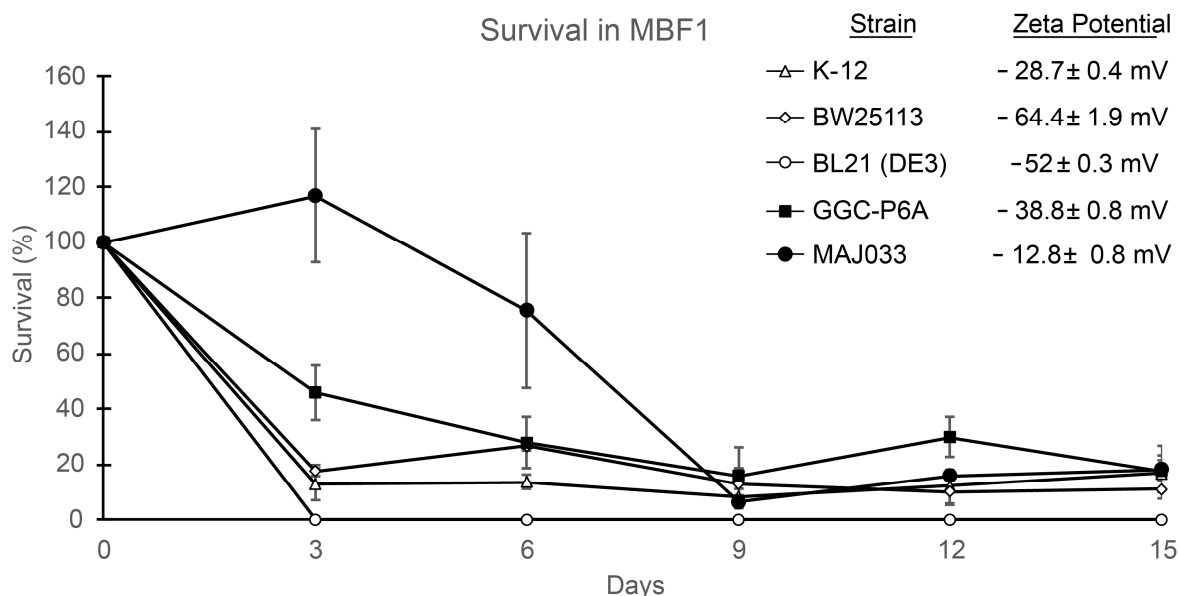


Figure 4. Percent survival of *Escherichia coli* strains K-12, BW25113, BL21 (DE3), MAJ033, and environmental isolate GGC-P6A in model paint with MBF1 over 15 days. Percent survival from model paint formulation following incubation at room temperature for 15 days. Plotted values are the average of three replicate binder solutions, with error bars representing standard deviation from the mean. Survival of BL21 (DE3) was not detected following day 0. Listed zeta potentials are averages of three replicate cultures.

Given that LPS is known to stabilize the Gram-negative outer membrane against environmental stresses, the lack of survival in BL21 (DE3) may be attributed to a truncated O-antigen. To determine if LPS altered the survival phenotype, we assayed survival in *E. coli* MAJ033, where a functional *wbbL* has been cloned into the K-12 background [33], and it demonstrated an overall change in surface charge (Figure 4). When this strain was assayed for survival in MBF1, the restoration of LPS synthesis demonstrated significantly higher culturability after inoculation compared to the other *E. coli* strains (Figure 4); however, survival was not significantly different from other strains after 9 days of incubation. This loss of viability after 9 days may be due to the lack of nutrients in the MBF1 paint formulation. Since the purpose of these experiments was to model commercial paint, we did not investigate whether the addition of nutrients promoted extended survival in this strain.

Since a robust genetic system exists for *E. coli*, using this strain gives us an opportunity to probe some of the other phenotypic determinants may contribute to the survival of bacteria in the paint environment using the Keio library (Figure 5) [25]. As screening for survival in the presence of an opaque model paint makes optical density measurements impossible, rather than screening the entirety of the Keio mutant strain library, we screened genes of interest using dilution plating. These genes included $\Delta rcsA$, as the B strain (BL21) lacks the ability to produce capsules due to the loss of the RcsA regulatory protein [34], leading to a complete loss of BL21 viability at 3 d in our initial survival assay (Figure 4). We selected $\Delta yhdH$ due to its role in acryloyl-CoA metabolism; the MBF1 solution is a styrene-acrylic latex, which could potentially be toxic due to the production of acryloyl-CoA during acrylate metabolism. Acryloyl-CoA is an electrophile that can interfere with electron transport [35], and mutants lacking the enzyme acryloyl-CoA reductase (*yhdH*) that converts acryloyl-CoA to the less toxic propionyl-CoA are more sensitive to acrylate [36]. Finally, we included $\Delta entA$, which lacks a gene necessary for synthesis of siderophores [37]. Since our model paint is a nutrient-poor environment, we wondered whether scavenging systems played an important role in the extended survival of *E. coli* strains. As controls, we used the WT host strain BW25113, along with two mutants we predicted would have no impact on survival: $\Delta mglA$, a subunit of the D-galactose/D-galactoside ABC transporter,

and $\Delta rfbD$ of the operon responsible for synthesizing the rhamnose component of the O-antigen, *rfbABCDX*. As we are not growing in the presence of galactose, and the K-12 background lacks a complete O-antigen, the deletion of either *mglA* or *rfbD* should have no observable phenotype in this assay. These mutant strains were incubated for 15 d at room temperature and the percentage survival (versus initial inoculum) was recorded (Figure 6). No significant difference in viability was observed between $\Delta mglA$ or $\Delta rfbD$ and BW25113. The survival of all three mutant strains ($\Delta rcsA$, $\Delta yhdH$, and $\Delta entA$) was significantly lower than WT, with the lowest occurring in $\Delta yhdH$, which is a mutation that affects acrylate metabolism (Figure 5). A one-directional ANOVA analysis [F(11,24) = 2.22, $p < 0.001$] indicated that the loss in viability of $\Delta entA$, $\Delta rscA$, and $\Delta yhdH$ was significant (Figure 6), indicating that the poor survival of *E. coli* strains may be due to cell surface chemistry, polymer toxicity, and nutrient limitation.

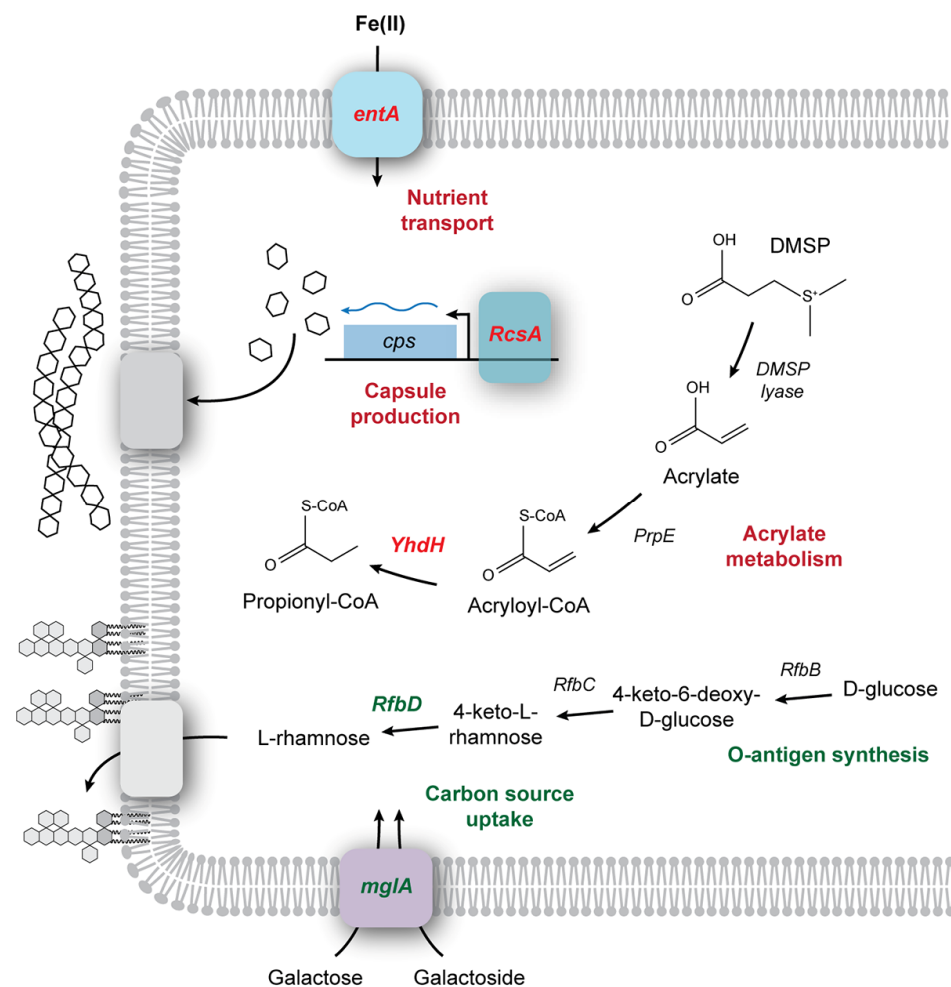


Figure 5. Genes in the *Escherichia coli* Keio library examined for their impact on survivability in a model paint formulation. Mutants in five genes (*entA*, *rscA*, *yhdH*, *rfbD*, and *mglA*) with known activities in membrane structure, nutrient uptake, or acrylate catabolism were tested. The paint formulation lacks nutrients for microbial growth, and a mutant in *entA*, which is involved in iron scavenging, demonstrated a reduction in survival. A mutation in *mglA*, which controls the uptake of glucose/galactoside that were not present in the paint formulation, had no impact on survival. Similarly, the *E. coli* K-12 strain does not produce O-antigen. A mutant in *rfbD*, which plays a critical role in O-antigen synthesis, had no impact on growth when compared to K-12. The *E. coli* str. BL21 lacks a capsule and demonstrated a reduction in long-term survival. A mutant lacking *rscA*, which is a positive regulator of capsule production, demonstrated similarly reduced survivability. Finally, acrylate in the paint could potentially be used for growth; however, the accumulation of the toxic

intermediate acryloyl-CoA would lead to cell damage. The *yhjH* mutant, which lacks the ability to detoxify acryloyl-CoA, led to a dramatic loss of cell viability, suggesting that acrylate metabolism was occurring. Genes with disrupted survival in paint are indicated in red, while those that had no significant effect on survival are shown in green. The basic functional pathway for the protein produced by each gene is shown; DMSP: dimethylsulfoniopropionate.

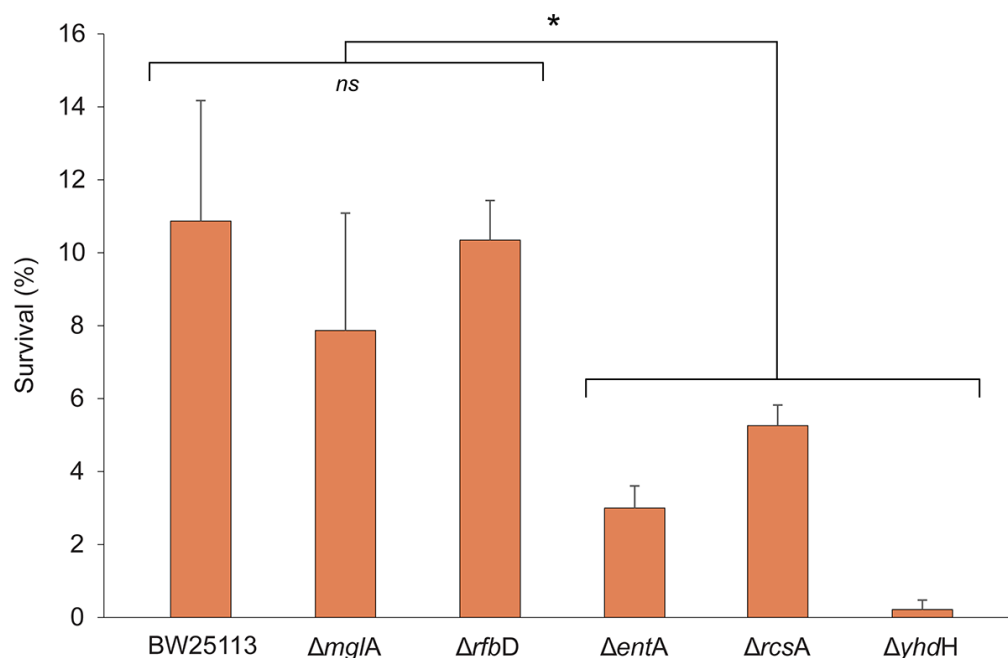


Figure 6. Percent survival of *Escherichia coli* knockout mutants in model paint with MBF1 over 15 days. Survival was calculated by comparing CFU/mL to values from day 0. Bars represent averages of three replicate cultures with bars showing standard deviation. Differences between survival rates were significant between groups according to a single factor ANOVA: $F(11,24) = 2.22$, $p < 0.001$. An asterisk (*) represents significantly lower survival compared to BW25113 (parent strain) using Tukey's Test; $df = 24$, $q = 4.63$. *ns* = not significant.

4. Discussion

In our past work, we observed that limestone (CaCO_3) cave environments contain bacterial species that use CaCO_3 precipitation to maintain Ca^{2+} homeostasis under what would otherwise be toxic levels [23]. The impact of this CaCO_3 precipitation in situ is the accumulation of microbially induced, centimeter-scale, secondary deposits known as cave popcorn [23]. Such secondary deposits can accumulate to many meters in length (stalactites and stalagmites) and occlude the original rock surface [23]. Coatings, including paints, often include CaCO_3 as a filler, which provides both color and appearance [14]. We therefore wondered whether added CaCO_3 could provide a source of Ca^{2+} ions to drive a similar precipitation process in coatings to generate a limited self-repair mechanism: a living paint. Toward this goal, we carried out proof-of-concept experiments to determine whether such bacteria could be successfully added to paints and coatings, remain viable through the formulation and film-forming process, and maintain a functional CaCO_3 precipitation phenotype to repair induced damage.

Water-based paint formulations contain a variety of organic polymers capable of supporting microbial growth. When sealed into a paint can, microbial anaerobic growth causes the degradation and spoilage of the paint formulation, including the release of unpleasant odors and potentially dangerous microbially derived volatile organic compounds [38–40]. The contamination of liquid formulations can also lead to substantial contamination of the final paint film, which can subsequently result in accelerated deterioration and discoloration [41,42]. While much work has attempted to identify the species responsible for this

growth, a range of species have been observed, and no work has attempted to identify the factors that allow for survival and growth in these chemistries [43]. Instead, most research (and patents) examining microbial survival in paint formulations has been geared toward limiting microbial (bacterial and fungal) survival and growth, either through the addition of biocides or formulation [41,44,45]. Our approach was to determine whether we could leverage microbial growth to generate a unique, engineered living material approach to improve the functionality of paint, while attempting to understand some of the factors that allow survival in a type bacterial species.

Our first step was to determine whether the bulk chemistry of paint would allow for the survival of our calcifying species. We examined the ability of 15 cave isolates (that demonstrated a strong calcifying phenotype [23]) to remain viable in three synthesized latex emulsions: MBF1, MBF2, and MBF3 (Table 1). Our original hypothesis was that the polymer chemistry would be the primary factor affecting cell viability, either through osmotic stress or charge effects on the surface of the polymer emulsions [46,47]. We expected a strong pattern of inhibition related to either the polymer chemistry or cellular structure of the target species (for example, binding effects related to Gram-negative or Gram-positive surface chemistries [46,47]), but no such pattern was observed. Rather, the data suggest that the impact of binder chemistry on viability may be related to species/strain genotype. Unsurprisingly, spore-forming bacteria maintained the greatest viability, with MBF1 (styrene–acrylic) being the most permissive to survival (Table 2). MBF3 is also a styrene–acrylic polymer, and this formulation was the least permissive to survival. In the monomeric form, styrene acts as an organic solvent that can reduce bacterial viability in the low mM range [48]. The mechanisms of styrene toxicity are unclear, although research suggests that styrene can remodel membrane fatty acids from the *cis* to the *trans* form via a general solvent stress response [48]. Given that we added cross-linking agents in excess (20%) during polymer synthesis, it is unlikely that unbound monomers reach the μM range (well below the toxicity observed for styrene), suggesting that styrene monomers alone are responsible for the observed loss of viability (Table 2; [49,50]). Another difference between MBF1 and MBF3 was the polymer cross-linking chemistry; MBF1 used diacetone acrylamide while Zn(II) was used for MBF3.

While acrylamide is an acute mutagen in eukaryotic cells, it has a reduced toxicity in bacteria [51], having been used successfully to encapsulate bacteria for a variety of industrial processes [52]. On the other hand, Zn(II) is known to be toxic [53], outcompeting Mg(II) cofactor binding sites and bringing about cell death by limiting essential cellular processes [54]. There are several ATP-driven transport pumps that detoxify cellular Zn(II); however, these tend to be plasmid-encoded, leading to strain and species variability (Table 2; [54,55]). We have previously demonstrated that cave-adapted microbial species display different sensitivities to transition metals [56], so the strain-specific sensitivity to MBF3 may reflect a differential sensitivity to Zn(II) rather than polymer chemistry.

Acrylates ($\text{CH}_2=\text{CHCOO}^-$) are found in relatively high abundance in nature, where they are formed from the catabolism of dimethylsulfoniopropionate (DMSP), an important organic compound in the sulfur cycle (Figure 5) [57]. As a result, the inhibitory levels of acrylates are relatively high (~ 30 mM; [58]). The ability to catabolize DMSP is dependent on the presence of the *ddd* genes, a group of DMSP lyases that cleave DMSP into 3-hydroxypropionate (3HP) and acrylate [58]. The next step in catabolism is the conversion of 3HP and acrylate to acryloyl-CoA, a strong electrophile capable of interfering with electron transport [36,57]. As a result, DMSP catabolism requires the cell to rapidly convert acryloyl-CoA to propionyl-CoA via acetyl-CoA reductase [36]. Genes involved in DMSP catabolism are widespread within bacterial species, even those species unlikely to be exposed to naturally occurring acrylates, including the genera *Bacilli* and *Microbacterium* (Table 2; [57,58]). Such pathways may therefore catabolize trace acrylate, with or without the cellular detoxification pathways necessary to remove acryloyl-CoA intermediates, as suggested by the $\Delta yhdH$ mutant [57]. The mutant $\Delta yhdH$ lacks a gene which encodes a protein with structural similarity to acryloyl-CoA reductase, *acuI* of *Ruegeria pomeroyi* [36],

and survival was dramatically reduced in $\Delta yhdH$ (Figure 6), suggesting that the ability to metabolize potentially toxic secondary products of acrylamide may be an important phenotype for strain viability in acrylate binders (Figure 5).

Given their chemically resistant nature, the GGC-P6A spores demonstrated greater long-term survivability than vegetative cells (Figure 2), and subsequent sampling demonstrated culturability in excess of 200 d. Nonetheless, any microbe added to a paint must be able to survive not only in the paint mixture, but the drying process once applied to a surface. When the liquid formula was inoculated and immediately drawn down into a paint film, both vegetative cells and spores remained viable through the drying process, but only the spore-containing formulations remained viable for 30+ days in films. When the dried films were placed on agar, microbial growth could be seen emerging from the edges of the film and along small cracks, suggesting that damage to the acrylic polymer may be necessary for the release of cells from entombment within the polymer, although direct access to nutrients in the agar matrix did not appear to be essential (Figure 3). This growth was quantified for GGC-P6A for 28 d (Figure 3), while the coupons contained viable spores for >1 year. Over time, a combination of microbial growth and CaCO_3 precipitation did lead to the occlusion of small cracks introduced into the paint film (Figure 3) with sufficient structural integrity that these films remained intact across the zone of repair when lifted from the plate. While the strength of this repair was not quantified, it does provide a level of self-healing that may be sufficient to protect the surface underneath and is a direction for future research. In all instances, microbial CaCO_3 precipitation continued to be observed in films, suggesting that the formulation, film-forming, and drying processes are permissive to maintaining this phenotype.

Very few of our original calcifying strains were Gram-negative bacteria. We thought that the outer lipid membrane would reduce viability in our formulations; however, when we used *E. coli* as a model organism, the data demonstrated viability for >15 d in MBF1. Nonetheless, there was variability in survival of the different *E. coli* strains. Given that polymer emulsions have a surface charge, we wondered whether the surface chemistry of the tested bacterial species was important for survival. To dissect the properties that could influence this survival, we examined the viability of several *E. coli* strains, along with mutants from the Keio library that differ significantly in membrane chemistry (Figure 4; K strains lack the O-antigen and B strains lack the ability to produce capsules) [34]. Our data did demonstrate a pattern of viability, and the restoration of LPS O-antigen synthesis (using *wbbL*⁺) improved survival, while the $\Delta rcsA$ mutant lacks ability to generate a capsule (similar to BL21; Figure 5) and had no detectable survival in our model paint, suggesting that the chemistry of the outer membrane is important for viability within paint. The gene *entA* is necessary for synthesis of the siderophore enterobactin [37] and $\Delta entA$ had a reduced survival rate in paint. While this could indicate that nutrient limitation may prevent extended survival, enterobactin also has a role in resistance to oxidative stress [59]. It is difficult to experimentally dissect these two interpretations in our system, especially as the addition of cationic Fe^{2+} ions will disrupt the emulsion chemistry. Nonetheless, the addition of nutrients to a formulated paint, which is often sealed for long-term storage, would in the very least be an extremely problematic mechanism of maintaining bacterial survival.

Our work has demonstrated the potential for an engineered living material that incorporates functional bacterial species into coatings and films. These data suggest that the impact of binder composition appeared to be strain-specific and that the polymer chemistry, cross-linking chemistry, and genotype of target species should all be considered when designing a coating that incorporates bacterial species. It is no surprise that spores survive for much longer in binders and liquid coatings, although it is unclear as to whether germination, growth, and subsequent germination occurs within the liquid paint formulation.

While our experiments suggest a self-healing paint that incorporates bacterial activity is possible, there are many obstacles that remain before a functional solution is possible. For example, the growth of microorganisms would need to be limited until self-healing is

initiated, preventing unwanted growth in stored paint, and Ca^{2+} ions within the paint film sufficient to support CaCO_3 precipitation and growth without the presence of a growth media/substrate remain elusive. Ongoing research will be required to examine ways to overcome these limitations.

Anthropogenic emissions of greenhouse gases represent one of the greatest threats to human society, with impacts on our climate that are expected to increase extreme weather events, reduce food production, reduce biodiversity, and damage important ecosystem services [60–64]. As society continues to shift toward sustainable production, there are many industries, such as construction, that are tied to products with few ‘green’ alternatives. While a self-healing coating does not remove the need for polymer synthesis, it could provide a cost-effective approach to reduce the number of applications and volume of paint needed to protect and maintain coated surfaces. The carbonates produced in our method are also fixed from atmospheric CO_2 , which does not require the movement of material from one site within a film to another to mediate repair that has been problematic in other proposed self-repair systems. Such CO_2 removal also provides for the possibility of carbon fixation in our approach, which has not been explored in any other microbially mediated self-healing approach.

5. Conclusions

Engineered living materials have the potential to revolutionize the construction industry, creating microbially augmented materials with self-healing capabilities. In coating systems, functional ELM materials have the potential to dramatically reduce maintenance costs. This work represents the first demonstration of the survival of bacterial species within latex emulsions commonly used in paints, demonstrating survival of spores for >28 days in the raw materials, liquid coating formulation, and dried films. Survival is not wholly contingent on spore formation but is influenced by a number of phenotypic properties, such as the ability to deal with the potentially toxic products from the metabolism of the polymer chemistry for growth. The most innovative aspect of the work was the demonstration that spores encapsulated in the polymer germinated and were able to grow and heal damage through the production of CaCO_3 in dried films. While this demonstration is far from a functional system for architectural paint, it does demonstrate the ability of embedded bacterial species to facilitate self-repair at the site of damage.

6. Patents

The work represented here formed the basis for the work contained within U.S. Patent: Self-repairing polymeric coatings, No. 11,396,604.

Supplementary Materials: The following supporting information can be downloaded at: <https://www.mdpi.com/article/10.3390/buildings14051202/s1>, Figure S1: Growth of *B. simplex* str. GGC-P6A in a model paint film made with the styrene–acrylic latex, MBF1; Figure S2: Scanning electron microscopy of paint films; Figure S3: Binder synthesis.

Author Contributions: Conceptualization, H.A.B.; methodology, M.E.J. and G.J.B.; formal analysis, H.A.B., M.E.J. and G.J.B.; methodology, M.E.J., G.J.B., A.D., C.T., A.K. and M.A.D.; writing—original draft preparation, M.E.J. and H.A.B.; writing—review and editing, H.A.B., M.E.J. and G.J.B.; supervision, H.A.B.; project administration, H.A.B.; funding acquisition, H.A.B. All authors have read and agreed to the published version of the manuscript.

Funding: This research was funded by the Defense Advanced Research Projects Agency (DARPA) Engineered Living Materials program under Agreement No. HR0011-18-9-0007. Approved for public release, distribution unlimited.

Data Availability Statement: The data presented in this study are available on request from the corresponding author H.A.B.

Acknowledgments: We would like to thank David Lowry and Adrian Tween for their technical assistance in this project, and Matt Jorgenson at the University of Arkansas for Medical Sciences for kindly providing the MAJ033 strain.

Conflicts of Interest: The authors declare no conflicts of interest. The funders had no role in the design of the study; in the collection, analyses, or interpretation of data; in the writing of the manuscript; or in the decision to publish the results.

References

1. Achal, V.; Mukherjee, A. A review of microbial precipitation for sustainable construction. *Constr. Build. Mater.* **2015**, *93*, 1224–1235. [[CrossRef](#)]
2. Peccia, J.; Kwan, S.E. Buildings, beneficial microbes, and health. *Trends Microbiol.* **2016**, *24*, 595–597. [[CrossRef](#)] [[PubMed](#)]
3. Heveran, C.M.; Williams, S.L.; Qiu, J.; Artier, J.; Hubler, M.H.; Cook, S.M.; Cameron, J.C.; Sruhar, W.V. Biomineralization and successive regeneration of engineered living building materials. *Matter* **2020**, *2*, 481–494. [[CrossRef](#)]
4. Wang, J.Y.; Soens, H.; Verstraete, W.; De Belie, N. Self-healing concrete by use of microencapsulated bacterial spores. *Cem. Concr. Res.* **2014**, *56*, 139–152. [[CrossRef](#)]
5. Nguyen, T.H.; Ghorbel, E.; Fares, H.; Cousture, A. Bacterial self-healing of concrete and durability assessment. *Cem. Concr. Compos.* **2019**, *104*, 103340. [[CrossRef](#)]
6. Anbu, P.; Kang, C.-H.; Shin, Y.-J.; So, J.-S. Formations of calcium carbonate minerals by bacteria and its multiple applications. *Springerplus* **2016**, *5*, 250. [[CrossRef](#)] [[PubMed](#)]
7. De Muynck, W.; De Belie, N.; Verstraete, W. Microbial carbonate precipitation in construction materials: A review. *Ecol. Eng.* **2010**, *36*, 118–136. [[CrossRef](#)]
8. Iqbal, D.M.; Wong, L.S.; Kong, S.Y. Bio-cementation in construction materials: A review. *Materials* **2021**, *14*, 2175. [[CrossRef](#)] [[PubMed](#)]
9. Stocks-Fischer, S.; Galinat, J.K.; Bang, S.S. Microbiological precipitation of CaCO₃. *Soil Biol. Biochem.* **1999**, *31*, 1563–1571. [[CrossRef](#)]
10. Gorospe, C.M.; Han, S.-H.; Kim, S.-G.; Park, J.-Y.; Kang, C.-H.; Jeong, J.-H.; So, J.-S. Effects of different calcium salts on calcium carbonate crystal formation by *Sporosarcina pasteurii* KCTC 3558. *Biotechnol. Bioprocess Eng.* **2013**, *18*, 903–908. [[CrossRef](#)]
11. Jonkers, H.M.; Thijssen, A.; Muyzer, G.; Copuroglu, O.; Schlangen, E. Application of bacteria as self-healing agent for the development of sustainable concrete. *Ecol. Eng.* **2010**, *36*, 230–235. [[CrossRef](#)]
12. Nguyen, P.Q.; Courchesne, N.M.D.; Duraj-Thatte, A.; Praveschotinunt, P.; Joshi, N.S. Engineered living materials: Prospects and challenges for using biological systems to direct the assembly of smart materials. *Adv. Mater.* **2018**, *30*, 1704847. [[CrossRef](#)] [[PubMed](#)]
13. Dhama, N.K.; Reddy, M.S.; Mukherjee, A. Biomineralization of calcium carbonates and their engineered applications: A review. *Front. Microbiol.* **2013**, *4*, 314. [[CrossRef](#)] [[PubMed](#)]
14. Streiberger, H.J.; Goldschmidt, A. *BASF Handbook: Basics of Coating Technology*, 3rd ed.; Vincentz Network: Hannover, Germany, 2018.
15. Hia, I.L.; Vahedi, V.; Pasbakhsh, P. Self-Healing Polymer Composites: Prospects, Challenges, and Applications. *Polym. Rev.* **2016**, *56*, 225–261. [[CrossRef](#)]
16. Song, Y.-K.; Chung, C.-M. Repeatable self-healing of a microcapsule-type protective coating. *Polym. Chem.* **2013**, *4*, 4940–4947. [[CrossRef](#)]
17. Suryanarayana, C.; Rao, K.C.; Kumar, D. Preparation and characterization of microcapsules containing linseed oil and its use in self-healing coatings. *Prog. Org. Coat.* **2008**, *63*, 72–78. [[CrossRef](#)]
18. Pungrasmi, W.; Intarasoontron, J.; Jongvivatsakul, P.; Likitlersuang, S. Evaluation of microencapsulation techniques for MICP bacterial spores applied in self-healing concrete. *Sci. Rep.* **2019**, *9*, 12484. [[CrossRef](#)]
19. Blaiszik, B.J.; Kramer, S.L.B.; Olugebefola, S.C.; Moore, J.S.; Sottos, N.R.; White, S.R. Self-Healing Polymers and Composites. *Annu. Rev. Mater. Res.* **2010**, *40*, 179–211. [[CrossRef](#)]
20. Selvarajoo, T. *Characterisation of a Vascular Self-Healing Cementitious Material System*; Cardiff University: Cardiff, UK, 2020.
21. Zhu, T.; Dittrich, M. Carbonate precipitation through microbial activities in natural environment, and their potential in biotechnology: A review. *Front. Bioeng. Biotechnol.* **2016**, *4*, 4. [[CrossRef](#)]
22. Mondal, S.; Ghosh, A.D. Review on microbial induced calcite precipitation mechanisms leading to bacterial selection for microbial concrete. *Constr. Build. Mater.* **2019**, *225*, 67–75. [[CrossRef](#)]
23. Banks, E.D.; Taylor, N.M.; Gulley, J.; Lubbers, B.R.; Giarrizo, J.G.; Bullen, H.A.; Hoehler, T.M.; Barton, H.A. Bacterial calcium carbonate precipitation in cave environments: A function of calcium homeostasis. *Geomicrobiol. J.* **2010**, *27*, 444–454. [[CrossRef](#)]
24. Ivey, D.M.; Guffanti, A.A.; Zemsky, J.; Pinner, E.; Karpel, R.; Padan, E.; Schuldiner, S.; Krulwich, T.A. Cloning and characterization of a putative Ca²⁺/H⁺ antiporter gene from *Escherichia coli* upon functional complementation of Na⁺/H⁺ antiporter-deficient strains by the overexpressed gene. *J. Biol. Chem.* **1993**, *268*, 11296–11303. [[CrossRef](#)]
25. Baba, T.; Ara, T.; Hasegawa, M.; Takai, Y.; Okumura, Y.; Baba, M.; Datsenko, K.A.; Tomita, M.; Wanner, B.L.; Mori, H. Construction of *Escherichia coli* K-12 in-frame, single-gene knockout mutants: The Keio collection. *Mol. Syst. Biol.* **2006**, *2*, 2006.0008. [[CrossRef](#)]

26. Breley, G.J.; Jennings, M.E.; Gisser, K.; Drabik, A.; Kainrad, J.; Barton, H.A. Techniques for quantifying bacterially induced carbonate mineralization in *Escherichia coli*. *Geomicrobiol. J.* **2023**, *40*, 88–99. [[CrossRef](#)]
27. Boquet, E.; Boronate, A.; Ramos-Cormenzana, A. Production of calcite (calcium carbonate) crystals by soil bacteria is a general phenomenon. *Nature* **1973**, *246*, 527–529. [[CrossRef](#)]
28. Anonymous. *Emulsion RV-LA*; Dow Chemical Company: Midland, MI, USA, 2010.
29. Anonymous. *Modifier AT-ER*; Dow Chemical Company: Midland, MI, USA, 2014.
30. Yoon, S.H.; Han, M.-J.; Jeong, H.; Lee, C.H.; Xia, X.-X.; Lee, D.-H.; Shim, J.H.; Lee, S.Y.; Oh, T.K.; Kim, J.F. Comparative multi-omics systems analysis of *Escherichia coli* strains B and K-12. *Genome Biol.* **2012**, *13*, R37. [[CrossRef](#)] [[PubMed](#)]
31. Lerouge, I.; Vanderleyden, J. O-antigen structural variation: Mechanisms and possible roles in animal/plant–microbe interactions. *FEMS Microbiol. Rev.* **2002**, *26*, 17–47. [[CrossRef](#)]
32. Jeong, H.; Barbe, V.; Lee, C.H.; Vallenet, D.; Yu, D.S.; Choi, S.-H.; Couloux, A.; Lee, S.-W.; Yoon, S.H.; Cattolico, L. Genome sequences of *Escherichia coli* B strains REL606 and BL21 (DE3). *J. Mol. Biol.* **2009**, *394*, 644–652. [[CrossRef](#)] [[PubMed](#)]
33. Browning, D.F.; Wells, T.J.; França, F.L.S.; Morris, F.C.; Sevastyanovich, Y.R.; Bryant, J.A.; Johnson, M.D.; Lund, P.A.; Cunningham, A.F.; Hobman, J.L. Laboratory adapted *Escherichia coli* K-12 becomes a pathogen of *C. aenorhabditis elegans* upon restoration of O antigen biosynthesis. *Mol. Microbiol.* **2013**, *87*, 939–950. [[CrossRef](#)]
34. Studier, F.W.; Daegelen, P.; Lenski, R.E.; Maslov, S.; Kim, J.F. Understanding the differences between genome sequences of *Escherichia coli* B strains REL606 and BL21 (DE3) and comparison of the *E. coli* B and K-12 genomes. *J. Mol. Biol.* **2009**, *394*, 653–680. [[CrossRef](#)]
35. Asao, M.; Alber, B.E. Acrylyl-coenzyme A reductase, an enzyme involved in the assimilation of 3-hydroxypropionate by *Rhodobacter sphaeroides*. *J. Bacteriol.* **2013**, *195*, 4716–4725. [[CrossRef](#)] [[PubMed](#)]
36. Todd, J.D.; Curson, A.R.J.; Sullivan, M.J.; Kirkwood, M.; Johnston, A.W.B. The *Ruegeria pomeroyi acul* gene has a role in DMSP catabolism and resembles *yhdH* of *E. coli* and other bacteria in conferring resistance to acrylate. *PLoS ONE* **2012**, *7*, e35947. [[CrossRef](#)]
37. Liu, J.; Duncan, K.; Walsh, C.T. Nucleotide sequence of a cluster of *Escherichia coli* enterobactin biosynthesis genes: Identification of *entA* and purification of its product 2, 3-dihydro-2, 3-dihydroxybenzoate dehydrogenase. *J. Bacteriol.* **1989**, *171*, 791–798. [[CrossRef](#)]
38. Oppermann, R.A.; Goll, M. Presence and effects of anaerobic bacteria in water-based paint. I. *JCT J. Coat. Technol.* **1984**, *56*, 51–56.
39. Norbäck, D.; Wieslander, G.; Ström, G.; Edling, C. Exposure to Volatile Organic Compounds of Microbial Origin (MVOC) during Indoor Application of Water-based Paints. *Indoor Air* **1995**, *5*, 166–170. [[CrossRef](#)]
40. Wieslander, G.; Norbäck, D. Ocular symptoms, tear film stability, nasal patency, and biomarkers in nasal lavage in indoor painters in relation to emissions from water-based paint. *Int. Arch. Occup. Environ. Health* **2010**, *83*, 733–741. [[CrossRef](#)] [[PubMed](#)]
41. Gaylarde, C.C.; Morton, L.H.G.; Loh, K.; Shirakawa, M.A. Biodeterioration of external architectural paint films—A review. *Int. Biodeterior. Biodegrad.* **2011**, *65*, 1189–1198. [[CrossRef](#)]
42. Ishfaq, S.; Ali, N.; Tauseef, I.; Khattak, M.N.K.; Shinwari, Z.K.; Ali, M.I. Analysis of paint degradation by fungal and bacterial species. *Pak. J. Bot.* **2015**, *47*, 753–760.
43. Obidi, O.F.; Aboaba, O.O.; Makanjuola, M.S.; Nwachukwu, S.C.U. Microbial evaluation and deterioration of paints and paint-products. *J. Environ. Biol.* **2009**, *30*, 835.
44. Maduka, C.M.; Igwilo, N.C. Microorganisms survive in paints. *Cur. Anal. Biotechnol* **2019**, *2*, 1–5.
45. Mutschlechner, M.; Walter, A.; Bach, K.; Schöbel, H. Beyond cultivation: Combining culture-dependent and culture-independent techniques to identify bacteria involved in paint spoilage. *Coatings* **2023**, *13*, 1055. [[CrossRef](#)]
46. Mankoci, S.; Kaiser, R.L.; Sahai, N.; Barton, H.A.; Joy, A. Bactericidal peptidomimetic polyurethanes with remarkable selectivity against *Escherichia coli*. *ACS Biomater. Sci. Eng.* **2017**, *3*, 2588–2597. [[CrossRef](#)] [[PubMed](#)]
47. Zander, Z.K.; Chen, P.; Hsu, Y.-H.; Dreger, N.Z.; Savariau, L.; McRoy, W.C.; Cerchiari, A.E.; Chambers, S.D.; Barton, H.A.; Becker, M.L. Post-fabrication QAC-functionalized thermoplastic polyurethane for contact-killing catheter applications. *Biomaterials* **2018**, *178*, 339–350. [[CrossRef](#)] [[PubMed](#)]
48. Sikkema, J.; de Bont, J.A.; Poolman, B. Mechanisms of membrane toxicity of hydrocarbons. *Microbiol. Rev.* **1995**, *59*, 201. [[CrossRef](#)] [[PubMed](#)]
49. Hartmans, S.; Van der Werf, M.J.; de Bont, J.A. Bacterial degradation of styrene involving a novel flavin adenine dinucleotide-dependent styrene monooxygenase. *Appl. Environ. Microbiol.* **1990**, *56*, 1347–1351. [[CrossRef](#)] [[PubMed](#)]
50. Van den Tweel, W.J.J.; Janssens, R.J.J.; De Bont, J.A.M. Degradation of 4-hydroxyphenylacetate by *Xanthobacter* 124X. *Antonie Van Leeuwenhoek* **1986**, *52*, 309–318. [[CrossRef](#)] [[PubMed](#)]
51. Tsuda, H.; Hamada, A.; Shimizu, C.S.; Kawata, K.M.; Hasegawa, M.M.; Taketomi, M.K.; Inui, N. Acrylamide; induction of DNA damage, chromosomal aberrations and cell transformation without gene mutations. *Mutagenesis* **1993**, *8*, 23–29. [[CrossRef](#)]
52. Cheetham, P.S.J. Developments in the immobilization of microbial cells and their applications. In *Topics in Enzyme and Fermentatino Biotechnology*; Wiseman, A., Ed.; Ellis Horwood Ltd.: New York, NY, USA, 1980; Volume 4, pp. 189–238.
53. Blencowe, D.K.; Morby, A.P. Zn(II) metabolism in prokaryotes. *FEMS Microbiol. Rev.* **2003**, *27*, 291–311. [[CrossRef](#)] [[PubMed](#)]
54. McDevitt, C.A.; Ogunniyi, A.D.; Valkov, E.; Lawrence, M.C.; Kobe, B.; McEwan, A.G.; Paton, J.C. A molecular mechanism for bacterial susceptibility to zinc. *PLoS Pathog.* **2011**, *7*, e1002357. [[CrossRef](#)]
55. Rosen, B.P. Bacterial resistance to heavy metals and metalloids. *JBIC J. Biol. Inorg. Chem.* **1996**, *1*, 273–277. [[CrossRef](#)]

56. Barton, M.D.; Petronio, M.; Giarrizzo, J.G.; Bowling, B.V.; Barton, H.A. The genome of *Pseudomonas fluorescens* strain R124 demonstrates phenotypic adaptation to the mineral environment. *J. Bacteriol.* **2013**, *195*, 4793–4803. [[CrossRef](#)] [[PubMed](#)]
57. Curson, A.R.J.; Todd, J.D.; Sullivan, M.J.; Johnston, A.W.B. Catabolism of dimethylsulphoniopropionate: Microorganisms, enzymes and genes. *Nat. Rev. Microbiol.* **2011**, *9*, 849. [[CrossRef](#)] [[PubMed](#)]
58. Curson, A.R.J.; Burns, O.J.; Voget, S.; Daniel, R.; Todd, J.D.; McInnis, K.; Wexler, M.; Johnston, A.W.B. Screening of metagenomic and genomic libraries reveals three classes of bacterial enzymes that overcome the toxicity of acrylate. *PLoS ONE* **2014**, *9*, e97660. [[CrossRef](#)] [[PubMed](#)]
59. Adler, C.; Corbalan, N.S.; Peralta, D.R.; Pomares, M.F.; de Cristóbal, R.E.; Vincent, P.A. The alternative role of enterobactin as an oxidative stress protector allows *Escherichia coli* colony development. *PLoS ONE* **2014**, *9*, e84734. [[CrossRef](#)] [[PubMed](#)]
60. Derocher, A.E.; Lunn, N.J.; Stirling, I. Polar bears in a warming climate. *Integr. Comp. Biol.* **2004**, *44*, 163–176. [[CrossRef](#)] [[PubMed](#)]
61. Jentsch, A.; Beierkuhnlein, C. Research frontiers in climate change: Effects of extreme meteorological events on ecosystems. *Comptes Rendus Geosci.* **2008**, *340*, 621–628. [[CrossRef](#)]
62. Lin, N.; Emanuel, K.; Oppenheimer, M.; Vanmarcke, E. Physically based assessment of hurricane surge threat under climate change. *Nat. Clim. Chang.* **2012**, *2*, 462–467. [[CrossRef](#)]
63. Parry, M.L.; Rosenzweig, C.; Iglesias, A.; Livermore, M.; Fischer, G. Effects of climate change on global food production under SRES emissions and socio-economic scenarios. *Glob. Environ. Chang.* **2004**, *14*, 53–67. [[CrossRef](#)]
64. Weiskopf, S.R.; Rubenstein, M.A.; Crozier, L.G.; Gaichas, S.; Griffis, R.; Halofsky, J.E.; Hyde, K.J.W.; Morelli, T.L.; Morissette, J.T.; Muñoz, R.C. Climate change effects on biodiversity, ecosystems, ecosystem services, and natural resource management in the United States. *Sci. Total Environ.* **2020**, *733*, 137782. [[CrossRef](#)]

Disclaimer/Publisher’s Note: The statements, opinions and data contained in all publications are solely those of the individual author(s) and contributor(s) and not of MDPI and/or the editor(s). MDPI and/or the editor(s) disclaim responsibility for any injury to people or property resulting from any ideas, methods, instructions or products referred to in the content.